Available online at www.sciencedirect.com
ScienceDirect
Chemical Engineering and Processing 46 (2007) 713–720
Chemical Engineering and Processing
www.elsevier.com/locate/cep

Steady state modeling of perforated plate extraction columns

R.S. Ettouney *, M.A. El-Rifai, A.O. Ghallab

Chemical Engineering Department, Faculty of Engineering, Cairo University, Giza, Egypt

Received 19 June 2006; received in revised form 23 September 2006; accepted 23 September 2006
Available online 7 November 2006

Abstract

A linear steady state model is developed for perforated plate liquid–liquid extractors conducting a slow pseudo first order reaction in the extract phase. The model assumes complete mixing of the continuous phase on each individual stage and plug flow of the uniformly sized dispersed phase droplets. An analytical relationship is developed to relate the achievable purification within a given number of actual plates in terms of three dimensionless parameters which are the extraction factor, a mass transfer rate factor, and a reaction rate enhancement factor. The developed model enabled the expression of the effect of the mass transfer and extraction factors on the overall cascade efficiency in the case of physical extraction and to demonstrate the qualitative and quantitative implications of the enhancing chemical reaction. It is also applicable in the analysis of the steady state control of the extract and raffinate product compositions in an existing column. In this case, the operating range constraints arising from the non-linear hydrodynamics relating the above three dimensionless parameters to the phase flow rates have to be considered.

Keywords: Perforated plate columns; Extractive reactors; Mixing models; Liquid–liquid extraction

1. Introduction

Modeling of heterogeneous fluid reactors involves the consideration of the fluid mixing patterns in formulating the conservation equations for each phase along with their appropriate boundary conditions, and the simultaneous application of physical equilibrium relations, inter-phase mass transfer rate expressions, and kinetic equations reflecting the mechanism and stoichiometry of the reaction. In continuous contact equipment, such as packed and spray columns, the contacting efficiency depends on the hydrodynamics and mixing characteristics within the phases. Plug flow and axial dispersion models have been used to study the steady-state [1], dynamic behaviour [2] and control [3] of continuous counter-current extractive reactors of various kinetics ranging between infinitely fast, pseudo first order, and second order reactions. Slow first order reactions conducted in mixer-settlers have been also studied assuming perfect mixing for the mixer, while various extents of mixing have been allowed with respect to both phases in the settler [4].

In equipment featuring complicated flow patterns such as pulsed and agitated extractors, cell models with inter-stage backflow have been proposed in order to consider the effect of the dispersed phase droplets size distribution, coalescence, and redispersion on the mass transfer efficiency. Models involving forward mixing led by drop size distribution and axial mixing of the continuous phase have been also suggested [5]. Recent models of extractive stirred column reactors are based on the droplet population balance model [6]. The bivariate droplet population balance model [7] uses computational fluid dynamics for describing the complex flows associated with droplet interactions such as breakage and coalescence, and axial transport [8,9] as well as the effects of inter phase mass transfer on viscosity, density, and interfacial tension [10]. A new approach to the application of population balance models relies on relatively straight forward single droplet experiments for incorporating the hydrodynamic characteristics into the model [11].

Un-agitated perforated plate extraction columns are of simple construction and suitable for conducting extractive reactions. These columns are appropriate for systems which are characterized by low interfacial tension and thus do not require mechanical agitation for good dispersion. They are effective both with respect to liquid handling capacity and extraction efficiency. This is because mixing within the continuous phase is confined to the holdup between individual trays, it does not spread through-

* Corresponding author. Tel.: +2 2 3301030/2 12 3149352; fax: +2 2 7346285.
E-mail addresses: ettouney@thewayout.net, rettouney@hotmail.com (R.S. Ettouney).

0255-2701/$ – see front matter © 2006 Elsevier B.V. All rights reserved.
doi:10.1016/j.cep.2006.09.007

out the tower from stage to stage, and because the tendency to establish concentration gradients within the droplets is avoided as the dispersed phase droplets coalesce and are reformed at each tray. Unlike pulsed and agitated column contactors, the hydrodynamic characteristics of perforated columns are relatively simple and fairly predictable by a number of existing correlations. This makes them amenable to a straightforward modeling approach.

The purpose of the present paper is to develop a steady state analysis of perforated plate extractive reactors modeled as a hybrid between staged and continuous contact equipment. The continuous phase on each plate is assumed to be well mixed and traversed by the dispersed phase droplets assumed in plug flow. Although pilot testing maybe required for finalizing design details of extraction equipment, a simple model would be useful in preliminary process analysis because the effects of the basic design and operating conditions are not overshadowed by system complexity. The developed model enables the expression of the column behaviour in terms of meaningful dimensionless parameters. It is applicable in the evaluation of alternative design configurations as well as in the analysis of the steady state response of existing perforated plate extractors subject to feed flow and/or composition disturbances.

2. The model system

A counter current un-agitated perforated plate extractive reactor is considered. The solute is transferred to the dispersed solvent phase where it undergoes a slow pseudo first order reaction with either the solvent itself or another dissolved reactant present in excess.

2.1. Assumptions

The following assumptions have been applied in the subsequent derivation:

1. The reacting solute is the only species transferred between the two immiscible phases. The transfer is according to a linear equilibrium relation:

$$y_n^* = mx_n \tag{1}$$

2. The reaction is confined to the solvent phase while heat and volume effects associated with the solute transfer and chemical reaction are negligible so that the interfacial tension, densities, and viscosities of the phases remain constant. Thus for given fixed values of the phase flow rates, the fractional holdup and overall solute mass transfer coefficient are the same for all plates.
3. Continuous phase liquid on a plate is perfectly mixed while the dispersed phase is in plug flow over the distance (h) between the plate and the coalesced layer of thickness (h_c) beneath the plate above.
4. The dispersed phase drops behave as spheres of uniform diameter, and no mass transfer takes place between the continuous phase and the coalesced solvent layer.

2.2. Model equations

Referring to Fig. 1, the solute undergoes a slow extractive reaction with the excess dispersed phase reactant which is insoluble in the continuous phase. The concentration (u) of this reactant remains therefore approximately constant throughout the column. Thus the reaction rate will be proportional to the concentration of the solute in the dispersed phase (y). Considering a plate (n) with effective contact height (h), a steady state material balance on the solute in an increment of height (dz) gives:

$$Vy + Ka'(y^* - y)A_a\phi_D\,dz = V(y + dy) + kyA_a\phi_D\,dz \tag{2}$$

Substituting from Eq. (1) and integrating between $z=0$ and $z=h$ gives,

$$\int_{n-1}^{n} \frac{dy}{Ka'mx_n - (Ka' + k)y} = \int_0^h \frac{A_a\phi_D\,dz}{V} \tag{3}$$

Which integrates to:

$$x_n = \frac{(1+\gamma)y_n - (1+\gamma)y_{n-1}e^{-\beta(1+\gamma)}}{m(1 - e^{-\beta(1+\gamma)})} \tag{4}$$

where:

$$\beta = \frac{Ka'A_a\phi_D h}{V} \quad \text{and} \quad \gamma = \frac{k}{Ka'}$$

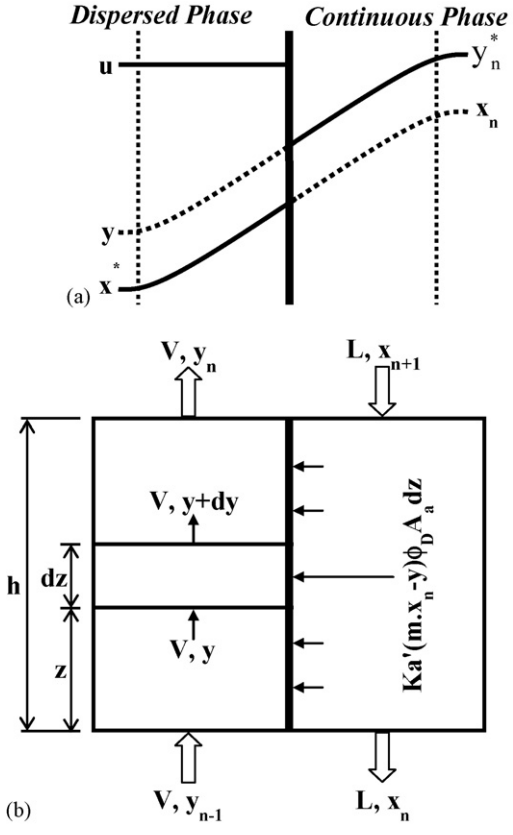

Fig. 1. Concentrations of excess dispersed phase reactant (u) and solute (x and y) across the interface at plate (n).

Referring to Fig. 1, a steady state material balance on the continuous phase gives:

$$L(x_{n+1} - x_n) - V(y_n - y_{n-1}) = \int_0^h ky\phi_D A_a \, dz \tag{5}$$

Substitution from Eqs. (1) and (2) shows that:

$$\int_0^h ky\phi_D A_a \, dz = \gamma V \int_{n-1}^n \frac{y \, dy}{mx_n - (1+\gamma)y} \tag{6}$$

Thus Eq. (5) integrates to:

$$V(y_n - y_{n-1}) - L(x_{n+1} - x_n) = \gamma V \left(\frac{(y_n - y_{n-1})}{(1+\gamma)} + \frac{mx_n}{(1+\gamma)^2} \ln \frac{mx_n - (1+\gamma)y_n}{mx_n - (1+\gamma)y_{n-1}} \right) \tag{7}$$

The combination of Eqs. (4) and (7) gives the second order difference equation,

$$y_{n+1} + by_n + cy_{n-1} = 0 \tag{8}$$

where:

$$b = -1 - e^{-\beta(1+\gamma)} - \frac{(1 - e^{-\beta(1+\gamma)})}{g(1+\gamma)^2} - \frac{\beta}{g} \frac{\gamma}{(1+\gamma)} \tag{9}$$

$$c = e^{-\beta(1+\gamma)} + \frac{(1 - e^{-\beta(1+\gamma)})}{g(1+\gamma)^2} + \frac{\beta}{g} \frac{\gamma}{(1+\gamma)} e^{-\beta(1+\gamma)} \tag{10}$$

$$g = \frac{L}{mV} \tag{11}$$

The boundary conditions at the feed end is given by:

$$x_{N+1} = x_f \tag{12}$$

Assuming a solute free solvent, the boundary condition at the solvent end is given by:

$$y_o = 0 \tag{13}$$

The solution of Eq. (8) subject to the boundary conditions of Eqs. (12) and (13) enables the expression of the ratio of the raffinate to feed compositions as:

$$\frac{x_1}{x_f} = \frac{p_1 - p_2}{p_1^{N+1} - p_2^{N+1} - e^{-\beta(1+\gamma)}(p_1^N - p_2^N)} \tag{14}$$

where p_1 and p_2 are the roots of the auxiliary quadratic: $p^2 + bp + c = 0$.

2.3. Estimation of model parameters

It is clear from the above model equations that the steady state behaviour of perforated plate extractive reactors is characterized by the three dimensionless parameters (g), (β), and (γ). The values of these parameters depend on the equilibrium partition and kinetic properties of the system (m and k), the operating flow rates (L and V), as well as on a number of plate design characteristics and system physico-chemical properties which affect the hydrodynamic performance of the column. Fairly reliable empirical correlations describing perforated plate hydrodynamics are well detailed in the literature [12–15]. They are applicable both for design of plate dimensions such as active area, downcomer area, net area, column diameter, and in analysis of the hydrodynamic performance for a given tray layout and operating flows. Fig. 2 outlines the computational sequence that has been used in the iterative solution of the hydrodynamic correlations for generating tray layout design data and/or in estimating the values of the hydrodynamic parameters for given plate dimensions. The sequence consists of six steps which will be briefly reviewed below.

In step 1 the hole velocity of the dispersed phase is computed. The optimum design value of the hole velocity depends on the perforation diameter (d_h), which usually ranges between $3\,m \times 10^{-3}$ m and $8\,m \times 10^{-3}$ m, the interfacial tension, and phase densities. The drop diameter is calculated in step 2, it is a function of the orifice diameter, actual orifice velocity, continuous phase viscosity in addition to phase densities and interfacial tension.

Step 3 deals with the calculation of the tray dimensions. The plate design should allow for stable hydrodynamics over a suitable range of phase flow rates. The downcomer area is based on ensuring that the downcomer velocity is low enough to avoid entrainment of droplets larger than about $7\,m \times 10^{-4}$ m and this depends on the continuous phase viscosity. The hole diameter, pitch, and downcomer area enable the calculation of the tower diameter hence the active area (A_a) and net area (A_n). The effective contact height (h) on a plate is calculated in step 4. Plate

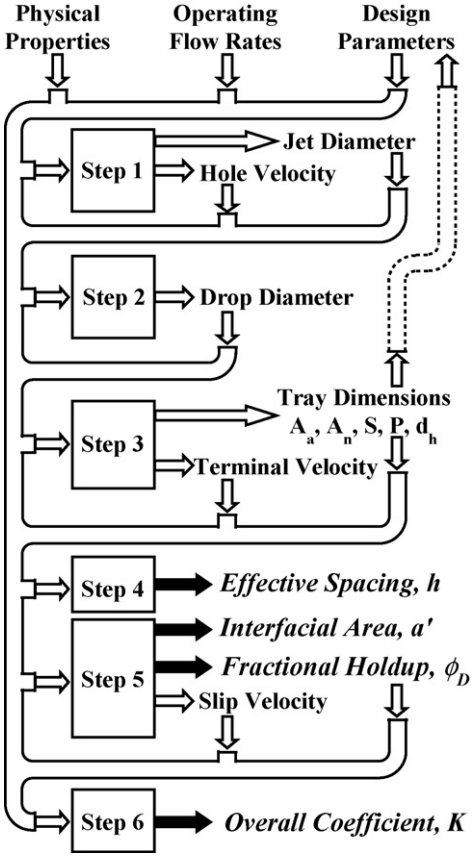

Fig. 2. Hydrodynamic and transport parameters computation scheme.

design data and phase flow rates enable the calculation of the continuous phase pressure drop through the downcomer and the dispersed phase pressure drop across the plate. The sum of these pressure drops is equivalent to the height of the coalesced layer (h_c) which when subtracted from the plate spacing (S) gives the value of (h) under the given operating conditions.

Holdup and slip velocity are calculated in step 5 in terms of the drop terminal velocity, dispersed phase flow rate, net plate area, drop diameter, phase densities, and viscosities. The dispersed phase holdup (ϕ_D) together with the drop diameter enable the estimation of (a'). The overall mass transfer coefficient is finally calculated in step 6 as a function of slip velocity, dispersed phase flow rate, fractional holdup, drop diameter, phase densities and viscosities, interfacial tension, solute partition coefficient, and solute diffusivities in the extract and raffinate films.

The above computational scheme maybe repetitively applied for the purpose of steady state control of an existing column. The non-linear empirical correlations are handled through straightforward MatLab programs. This enables the online estimation of the values of (h), (ϕ_D), (a'), (K), and hence the dimensionless parameters (g, β, and γ) in terms of the phase flow rates.

3. Application to Design

Eq. (14) maybe used to calculate the number of actual stages required to effect a given separation task. It relates the purification obtainable in a (N) perforated plate extractive reactor to the three dimensionless parameters (g, β, and γ). The extraction factor (g) is the ratio between the slopes of the operating line and equilibrium relation; (β) is a dimensionless mass transfer parameter which reflects the ratio between the mass transfer rate constant and the dispersed phase space velocity on a stage; while (γ) is a dimensionless enhancement factor giving the ratio between the reaction rate constant and the mass transfer rate constant.

3.1. Physical Extraction

In case of purely physical extraction, (γ) equals zero and the system performance will be governed by the two parameters (g) and (β). A graphical display of the relation between (x_1/x_f), (N), (g), and (β) as given by Eq. (14) may simplify repetitive preliminary process design and costing calculations. In case of theoretical stages and solute free solvent feed, the Kremser equation [16] relates the purification ratio (x_1/x_f) to the number of theoretical stages (N_t) by:

$$\frac{x_1}{x_f} = \frac{g^{N_t+1} - g^{N_t}}{g^{N_t+1} - 1} \tag{15}$$

This enables the display on a single chart of the relative enrichment or depletion versus the number of theoretical stages with the extraction or stripping factor (g) as a parameter [17]. In the case of actual stages, an additional mass transfer parameter (β) is involved to reflect the effect of system hydrodynamics and transport properties on the overall cascade efficiency.

The combination of Eqs. (14) and (15) enables the calculation of the overall cascade efficiency in terms of (g), (β), and (N_t).

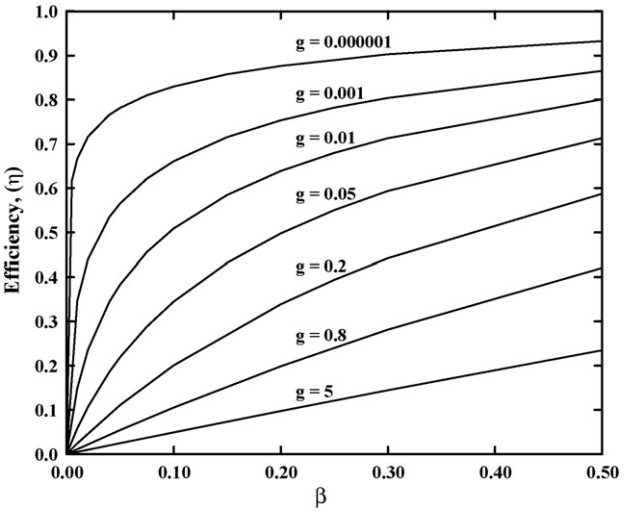

Fig. 3. Effects of extraction factor and mass transfer parameter on overall column efficiency.

Analysis of Eqs. (14) and (15) indicates that in the case of physical extraction (i.e. when $\gamma = 0$), the overall cascade efficiency (N_t/N) is independent of the purification ratio or the total number of stages. Fig. 3 displays the computed overall cascade efficiency in terms of the extraction factor (g) and the dimensionless mass transfer parameter (β). A quick estimation of the number of actual stages may be thus obtained from the standard theoretical stage chart [12,17] and multiplication by an efficiency factor. For simplicity, the data on Fig. 3 has been correlated in the form of the equation:

$$\eta = 1 - e^{-\alpha\beta^r} \tag{16}$$

where (α) and (r) depend on the extraction factor (g) and are obtainable from Fig. 4.

3.2. Effect of chemical reaction

When the solute is depleted by a chemical reaction in the extract phase (i.e. when $\gamma \neq 0$), the ratio between the numbers

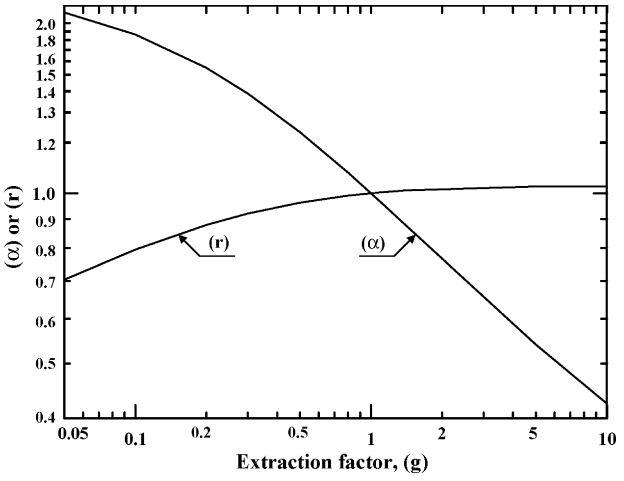

Fig. 4. Correlation parameters (r) and (α) as functions of the extraction factor, (g).

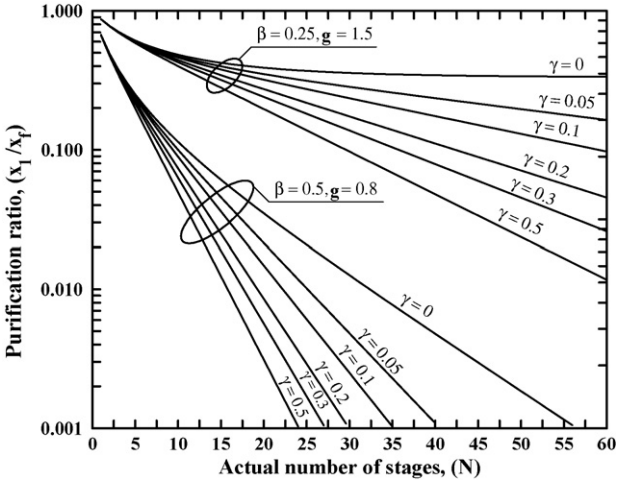

Fig. 5. Effect of chemical reaction in enhancing extraction for two sets of values of (β) and (g).

of actual and theoretical equilibrium stages is not independent of the targeted purification ratio. This means that the system would not lend itself to a straightforward efficiency correlation as was the case with physical extraction. Application of Eq. (14) indicates that the required number of actual plates decreases with the decrease of (g) and the increase of (β) as was the case with purely physical extraction. It also decreases with the increase of (γ). The effect of the chemical reaction in enhancing extraction is illustrated in Fig. 5.

Another effect of the presence of a chemical reaction is that it enables the realization of a purification ratio beyond that obtainable with an infinite number of equilibrium stages in the case of purely physical extraction when ($g > 1$). Eq. (15) gives the minimum raffinate composition for a given extraction factor as:

$$\underset{N_t \to \infty}{\text{Lt}} \frac{x_1}{x_f} = 1 - \frac{1}{g}, \quad \text{for } g > 1 \tag{17}$$

$$\underset{N_t \to \infty}{\text{Lt}} \frac{x_1}{x_f} = 0, \quad \text{for } g \leq 1 \tag{18}$$

This limiting condition of infinite number of stages also corresponds to minimum solvent requirements and maximum extract composition. Fig. 6 shows that for ($g < 1$) the number of actual stages is higher than the number of equilibrium stages. For ($g > 1$), the chemical reaction enables the removal of the minimum purification ratio constraint associated with physical extraction.

The effect of chemical reaction is also illustrated by considering the evolution of the continuous phase composition along an extractive reactor. Fig. 7 compares these composition profiles for three cases. It is seen that for the given values of (g, β, and γ) and the specified purification task, the overall column efficiency with respect to equilibrium stages is about 37.2% in absence of chemical reaction and about 89.2% in the presence of a chemical reaction.

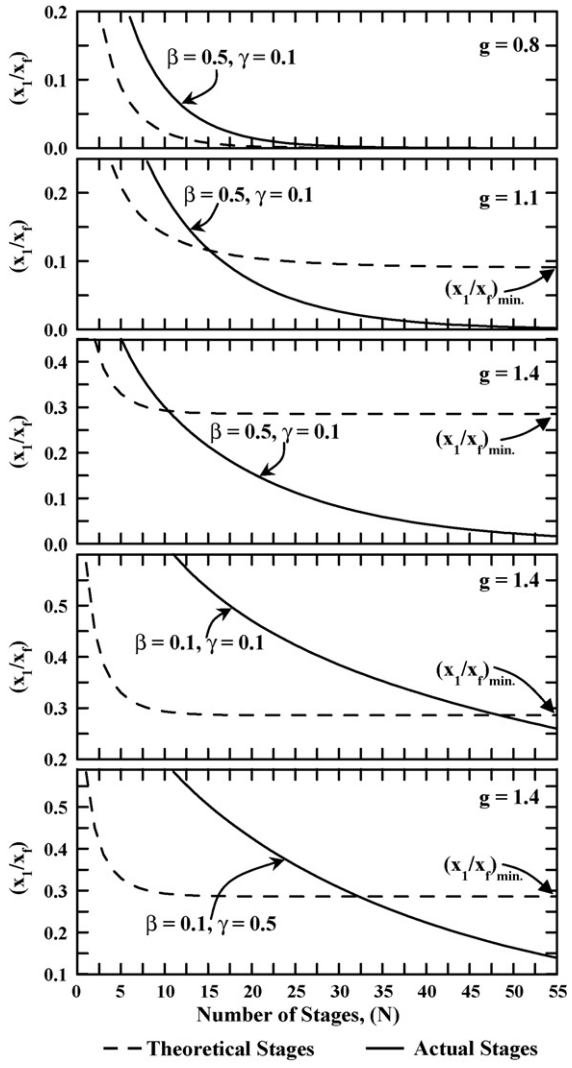

Fig. 6. Comparison of performance of equilibrium and actual stages for different values of (g), (β), and (γ).

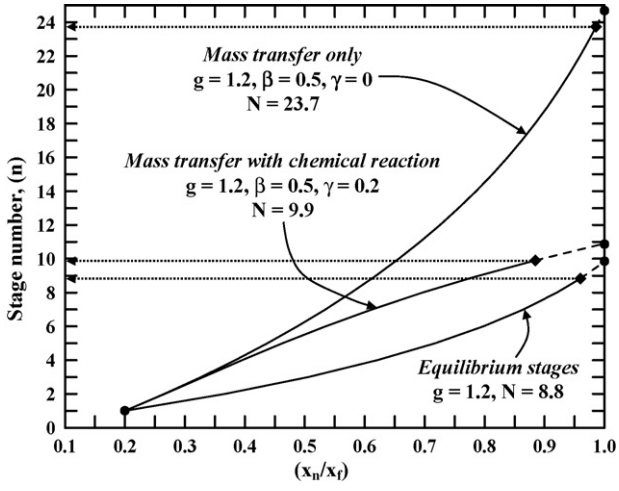

Fig. 7. Effect of mass transfer and chemical reaction on the number of stages and continuous phase composition profiles.

4. Column control

In order to secure stable phase contacting patterns and efficient mass transfer, the phase flow rates should be within appropriate ranges. The dispersed phase flow rate should correspond to hole velocities ranging between 0.1 m/s and 0.15 m/s. The thickness of the coalesced layer below a plate should not be less than about 0.05 m of the dispersed phase liquid. This thickness corresponds to the sum of the pressure drops of the dispersed phase across a plate and that of the continuous phase in its downcomer. This fixes the lower limit on the continuous phase flow rate. The upper limit on the continuous phase flow rate is not only governed by entrainment considerations as explained in Section 2.3 but also by pressure drop considerations. The continuous phase pressure drop should not lead to an unduly high thickness of the coalesced layer since this results in a reduction of the effective contact height.

The hydrodynamic and transport parameters in a column of given number of plates and plate design are non-linearly related to the phase flow rates. They may be estimated from the empirical correlations reviewed in Section 2.3. For perforated plate columns, the holdup, slip velocity, volumetric mass transfer coefficient, and drop diameter are functions of the dispersed phase flow rate only. On the other hand, the effective plate contact height (h), and the parameters (β), (g), and (γ) depend on the flow rates of both phases. Since the parameters (β), (g), and (γ) depend on column hydrodynamics, any change in the phase flow rates is immediately reflected on the column efficiency and hence on the obtained purification ratio. Fig. 8 illustrates the effect of phase flow rates on (β) for a column of fixed plate design.

When an existing column with a given plate design is subjected to disturbances in the feed composition (x_f) and/or feed flow rate (L), the desired raffinate product composition (x_1) may be restored by manipulating the solvent phase flow rate (V). Fig. 9 displays the results of the computations of the ratio (x_1/x_f) as a function of both (L) and (V) for the studied column taking into account the variation of column efficiency with the phase flow rates. For the studied column, the operating range of the phase flow rates is within ± 25% of the nominal design value i.e. between 0.0022 m^3/s and 0.003 m^3/s for the continuous phase and between 0.0075 m^3/s and 0.013 m^3/s for the dispersed phase. Point (1) on Fig. 9 corresponds to the desired value of $x_1 = 0.6$ kmol/m^3, a feed composition $x_f = 2.911$ kmol/m^3, i.e. $x_1/x_f = 0.2061$, and the operating conditions $L = 0.0022$ m^3/s and $V = 0.0076$ m^3/s. Assuming that the continuous phase flow rate, (L) increases to 0.0026 m^3/s and that the feed composition, (x_f) increases simultaneously to 4.386 kmol/m^3, and it is required to maintain the desired raffinate composition of 0.6 kmol/m^3, i.e. $x_1/x_f = 0.1368$, the solvent flow rate, (V) has to be increased to 0.0106 m^3/s as indicated by point (2) on the diagram. Measurements of (L) and (x_f) enable the computation of the solvent throughput (V) required to maintain the desired value of the raffinate composition (x_1).

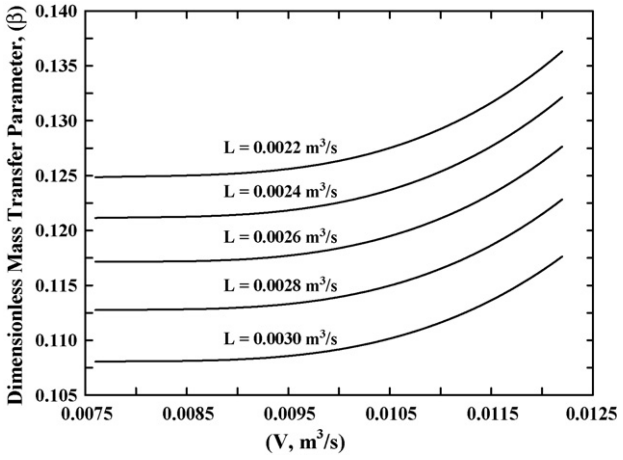

Fig. 8. Effect of phase flow rates on (β).

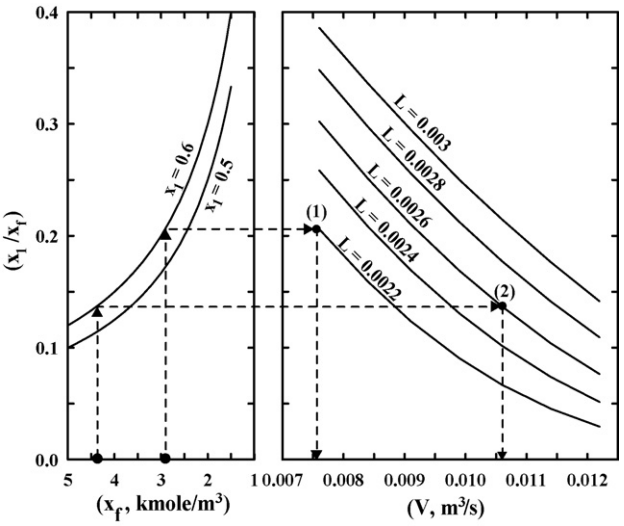

Fig. 9. Steady state control of raffinate composition by manipulation of solvent flow rate.

If both extract and raffinate compositions are to be maintained despite disturbances in the feed composition, both the feed and solvent flow rates have to be manipulated. The range within which both (L) and (V) can be varied depends on the constraints dictated by column hydrodynamics. The relation between (L) and (V) satisfying the computed value of (x_1/x_f) is directly obtainable from the data presented in Fig. 9 and is shown in Fig. 10. In the case of physical extraction the relationship between (L) and (V) satisfying the desired values of (x_1) and (y_N) for the measured value of (x_f) is obtainable by an overall material balance on the column which gives:

$$L = \frac{y_N/x_1}{[(x_f/x_1) - 1]} V \tag{19}$$

When the ($L - V - x_1/x_f$) relations shown in Fig. 10 are simultaneously solved with the straight lines of Eq. (19), the admissible ranges of (y_N/x_1) may be obtained as a function of (x_1/x_f) as shown in Fig. 11. The upper curve on Fig. 11 corresponds to the lower phase flow rate constraints represented by circular points on Fig. 10, while the lower curve on Fig. 11 corresponds to the higher phase flow rates represented by the square points on Fig. 10. It is seen that the constraints on the phase flow rates limit the admissible choices of (y_N) for a given (x_1) within narrow ranges depending on the

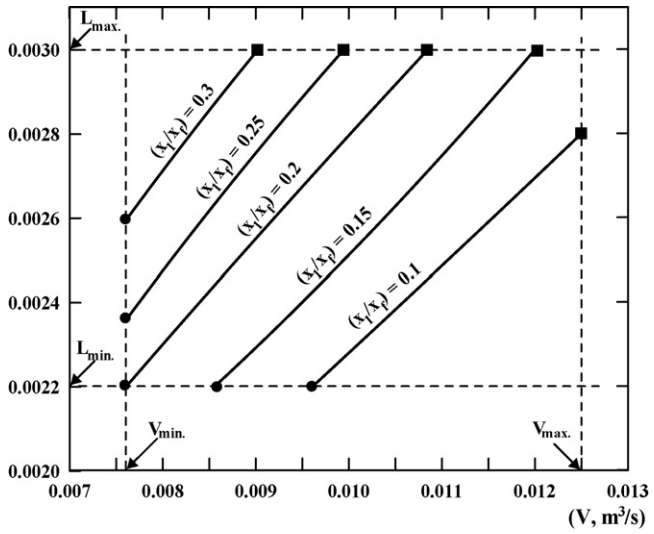

Fig. 10. Effect of the purification ratio on the relation between admissible continuous and dispersed phase flow rates.

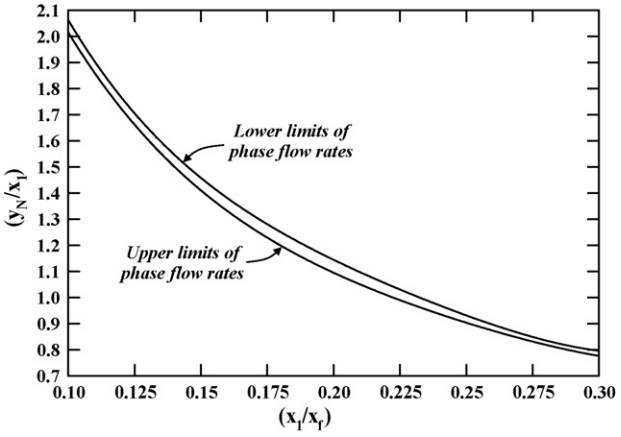

Fig. 11. Admissible ranges for the ratio of set points of extract and raffinate compositions.

value of (x_f). Thus for $x_1 = 0.6\,kmol/m^3$, and $x_f = 3\,kmol/m^3$, i.e. $(x_1/x_f) = 0.2$, the maximum and minimum allowable values of (y_N) are 0.687 kmol/m^3 and 0.656 kmol/m^3, respectively. For $(y_N) = 0.687\,kmol/m^3$, the phase flow rates are to be manipulated to the values $L = 0.0022\,m^3/s$ and $V = 0.0076\,m^3/s$, while for $(y_N) = 0.656\,kmol/m^3$ the continuous and dispersed phase flow rates should be maintained at $L = 0.003\,m^3/s$ and $V = 0.011\,m^3/s$, respectively.

5. Conclusions

1. Perforated plate liquid–liquid extractors feature simple construction, relatively stable phase contacting patterns, and limited axial mixing along the column. They are amenable to a relatively straightforward steady state analysis of their behaviour. This enabled the development of a simple model where the effect of the basic design and operating conditions is not overshadowed by system complexity.
2. An individual stage model assuming plug flow of the dispersed phase, complete back mixing of the continuous phase, linear equilibrium relation, and a pseudo first order dispersed phase reaction has been derived and generalized to describe the cascade behaviour in terms of actual number of stages and three dimensionless parameters reflecting the effects of operating conditions, contacting efficiency, and chemical reaction.
3. In the case of physical extraction, the overall efficiency of the cascade is independent of the number of stages and has been correlated as a function of the extraction factor (g) and the mass transfer parameter (β) only.
4. The effect of presence of a chemical reaction is to improve the overall cascade efficiency. It also enables to obtain a raffinate product composition below the minimum value obtainable with an infinite number of equilibrium stages at extraction factors above 1.0.
5. The application of the developed model to the analysis of the steady state performance and control of an existing column incorporates the effect of change in phase flow rates on the hydrodynamic and mass transfer characteristics of the column. During operation, such changes may either occur as disturbances or be deliberately effected for the purpose of composition control. A scheme for computing the flow rate manipulations required to respond to performance requirements is illustrated through an example.

Appendix A. Nomenclature

a'	interfacial area per unit volume of dispersed phase (m^2/m^3)
A_a	active plate perforated area (m^2)
A_n	net tower area (m^2)
b	dimensionless parameter given by Eq. (9)
c	dimensionless parameter given by Eq. (10)
d_h	hole diameter (m)
D_p	droplet diameter (m)
g	extraction factor (L/mV)
h	effective stage height (m), $h = S - h_c$
h_c	height of coalesced layer (m)
k	reaction rate constant (s^{-1})
K	mass transfer coefficient (m/s)
L	volumetric flow rate of the continuous phase (m^3/s)
m	slope of the equilibrium relation
N	number of actual perforated plates
N_t	number of theoretical plates
P	pitch (m)
p_1, p_2	roots of the auxiliary quadratic equation, $p^2 + bp + c = 0$
r	dimensionless parameter in efficiency correlation, Eq. (16)
S	tray spacing (m)
u	solvent phase reactant concentration ($kmol/m^3$)
v_s	slip velocity (m/s)
V	volumetric flow rate of the dispersed phase (m^3/s)
x	solute concentration in the continuous phase ($kmol/m^3$)
x_1	solute concentration in the final raffinate ($kmol/m^3$)

x_f solute concentration in the continuous phase feed (kmol/m^3)
y solute concentration in the dispersed phase (kmol/m^3)
y_o solute concentration in the fresh solvent (kmol/m^3)
y_N solute concentration in the final extract (kmol/m^3)
y_n^* dispersed phase concentration in equilibrium with a continuous phase concentration x_n (kmol/m^3)

Greek letters
α dimensionless parameter in efficiency correlation, Eq. (16)
β dimensionless mass transfer parameter, $Ka' A_a \phi_D h/V$
ϕ_D dispersed phase holdup
γ dimensionless enhancement factor, k/Ka'
η overall cascade efficiency

References

[1] M.A. El-Rifai, S.S.E.H. El Nashaie, A.A. Kafafi, Analysis of a countercurrent tallow-splitting column, Trans. Inst. Chem. Eng. 55 (1977) 59–63.
[2] S.S.E.H. El Nashaie, M.A. El-Rifai, M.N. Abd El-Hakim, Effect of kinetic regime and axial dispersion on the dynamic response of counter flow extractive reactors, Chem. Eng. Sci. 33 (1978) 847–852.
[3] M.A. El-Rifai, S.S.E.H. El Nashaie, M.N. Abd El-Hakim, Composition dynamics and control in counter flow extractive reactors, in: Proceedings of the Cairo International IFAC Conference on systems approach for development, Pergamon Press, 1977, pp. 315–320.
[4] M.A. El-Rifai, Composition dynamics in multi-mixer-settler extractive reaction batteries, Chem. Eng. Sci. 30 (2) (1975) 79–87.
[5] V. Rod, Calculating mass transfer with longitudinal mixing, Br. Chem. Eng. 11 (6) (1966) 483–490.
[6] H.J. Bart, Reactive extraction- status report on the simulation of stirred columns, Chem. Ing. Tech. 74 (3) (2002) 229–241.
[7] S.A. Schmidt, M. Simon, M.M. Attarakih, L. Lagar, H.J. Bart, Droplet population balance modeling, hydrodynamics and mass transfer, Chem. Eng. Sci. 61 (1) (2006) 246–256.
[8] T. Kronberger, A. Ortner, W. Zulehner, H.J. Bart, Numerical simulation of extraction columns using a drop population model, Comput. Chem. Eng. 19 (1) (1995) 639–644.
[9] H.J. Bart, Reactive extraction in stirred columns—a review, Chem. Eng. Technol. 26 (7) (2003) 723–731.
[10] M.M. Attarakih, H.J. Bart, N.M. Faqir, Numerical solution of the bivariate population balance equation for the interacting hydrodynamics and mass transfer in liquid–liquid extraction columns, Chem. Eng. Sci. 61 (1) (2006) 113–123.
[11] H.J. Bart, From single droplet to column design, Tsinghua Sci. Tech. 11 (2) (2006) 212–216.
[12] R.E. Treybal, Mass Transfer Operations, third ed., McGraw Hill International Editions, 1981, pp. 530–541.
[13] D. Mewes, Th. Pilhofer, Prediction of fluid dynamic properties of unpulsed sieve plate extraction columns, Ger. Chem. Eng. 2 (1979) 69–76.
[14] H.-J. Bart, Reactive Extraction, Springer Series: Heat and Mass Transfer, Berlin, (2001) 156–168.
[15] L.A. Robbins, R.W. Cussack, Liquid–Liquid Extraction, Operations and Equipment, Section 15, Perry's Chemical Engineers' Handbook, seventh ed., McGraw Hill, New York, 1997.
[16] A. Kremser, Theoretical analysis of absorption process, Nat. Pet. News 22 (21) (1930) 48–52.
[17] J.M. Douglas, Conceptual Design of Chemical Processes, McGraw-Hill, 1988, p.428.